Applied Mechanics and Materials *Online: 2013-11-08*
ISSN: 1662-7482, Vols. 446-447, pp 452-457
doi:10.4028/www.scientific.net/AMM.446-447.452

Computation of Hoisting Forces on Wind Turbine Blades using Computation Fluid Dynamics

Wang Yong [a], Tian De[b], and He Wei[c]

Renewable Energy School, North China Electric Power University, Beijing, China

[a]wangyyong100@163.com, [b]tiande@ncepu.edu.cn, [c]lanlyhw@163.com

Keywords: Wind Turbine, Hoisting Force, Blade Position, CFD.

Abstract. The hoisting forces on a 38.5m wind turbine blade in multiple positions are computed using the computational fluid dynamics (CFD) method. The computation model is constructed with the steady wind conditions, blade mesh model and the blade positions which are determined by the blade pitch angle, azimuth angle and rotor yaw angle. The maximal and minimal hoisting forces in three-dimensional coordinates are found and the corresponding pitch angle, azimuth angle and yaw angle are obtained. The change of the hoisting forces on wind turbine blades is analyzed. Suggestions are given to decrease the hoisting forces of the blade in open wind environment.

Introduction

The wind turbine is the fundamental machine to convert wind energy into mechanical energy and electricity. To improve the efficiency and robustness and reduce the costs of design, manufacturing, assembly and maintenance of wind turbines, wind turbine technologies are studied by many scholars and researchers. These focuses include aerodynamics characteristics [1] of wind turbine blades, wind turbine design and optimization [2] and wind turbine control [3], etc. Among these research topics, the assembly and installation process of wind turbines are seldom considered. The assembly and installation of wind turbines occur at the rear stage of wind turbine manufacturing. The hoisting process of some components, such as the blades, rotors and nacelles, is different from that of the products in the workshop. Due to the aerodynamic characteristics of the blades, the hoisting process of wind turbine blades and rotors in the wind farm is affected by the wind speed and directions. By identifying the change of the hoisting forces of blades in wind farm, the CFD method is used to compute the hoisting forces of blades in different positions. The blade positions are concluded by the blade pitch angle, azimuth angle and rotor yaw angle.

The wind speed, the temperature and the atmosphere moisture, etc play an important role to affect the hoisting process of wind turbine blades. The restrictive conditions for wind turbine assembly and installation are introduced in the guidelines [4]. The hoisting difficulty and safety of wind turbine blades is mostly impacted by the wind speed due to their good aerodynamic characteristics [5]. Once the wind speed exceeds 10m/s on average, the hoisting process of blades must be stopped.

The fluctuation of hoisting forces of wind turbine blades is mainly determined by the aerodynamic forces. The aerodynamic forces of a blade in the hoisting process are concluded by the blade positions which are represented as the blade pitch angle, azimuth angle and rotor yaw angle. With the same wind speed, the hoisting forces vary according to the positions of the blade. The minimum hoisting force is beneficial to improve the safety and efficiency of the hoisting process and the blade positions are taken into account by the engineers to make the best plans of the hoisting process.

The CFD method is widely used to simulate the aerodynamic behavior of wind turbines. Cochran et al [6] pointed out that computation of wind engineering has become a commonplace method to complement, eventually replace physical modeling. But they are seldom done for the hoisting process of wind turbine and the relationships between the hoisting forces and the blade positions are seldom considered. This research tries to illuminate the problem with CFD method. Due to the complexity of wind conditions, only steady wind conditions are used and the hoisting forces in particular positions

of blades are computed accurately. The change of hoisting forces of the wind turbine blade is analyzed. The minimal hoisting forces and the corresponding blade positions are obtained.

The Computation Model

To benefit the following description, some abbreviations are defined. PA, AA and YA represents blade pitch angle, azimuth angle the rotor yaw angle. *BX*, *BY* and *BZ* are the *x*, *y* and *z* coordinate axis of blade coordinate. The hoisting forces of blades change with the angle between the wind direction and blade positions. The blade positions are represented as the PA, AA and YA. The yaw coordinate system is considered as the global coordinate system and the yaw angles are computed according to this coordinate. The aerodynamic forces on the blades are computed with respect to the yaw coordinate system and the hoisting forces *F*x, *Fy* and *Fz* are their balance forces plus the blade weight.

To ensure the balance of the rotor in the hoisting process, the position in Fig. 1 is frequently used. In Fig. 1, the AAs of blade 1, blade 2 and blade 3 are 0^0, 120^0, -120^0, respectively. For each blade, the YA interval is assigned as [0^0, 360^0] which is divided into 12 portions. The degree between two adjacent yaw positions is 30^0. The YA division is shown in Fig. 2. For the appointed AA and YA, the blade PA changes from -90^0 to 90^0. The blade PA interval is assigned as [-90^0, 90^0] which is divided into 6 portions as shown in Fig. 3. The datum of blade positions is listed in Table 1.

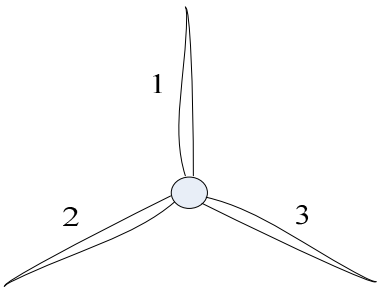

Fig. 1 The rotor position

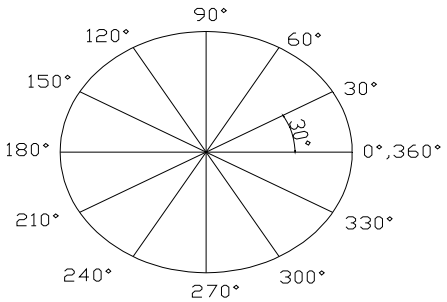

Fig. 2 The yaw angle division

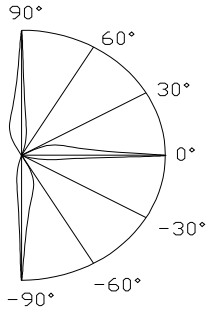

Fig.3 The pitch angle division

Table 1 The blade positions in Fig. 1

Blade		Blade 1	Blade 2	Blade 3
Positions	AA/ ^{0}	0	-120	120
	PA/ ^{0}	-90~90	-90~90	-90~90
	YA/ ^{0}	0~360	0~360	0~360

For each blade in Fig. 1, there are 84 hoisting forces to be computed based on the 12 YAs × 7 PAs. Therefore, a total of 252 hoisting forces are computed for the three blades in Fig. 1. The maximal and minimal hoisting forces of each blade are derived from the change of the hoisting forces and the corresponding positions of the blades will be obtained.

The dimensions and mass of the blade and hub is listed in Table 2. The blade model originates from literature [7]. The blade airfoils come from NREL [8-9] and the geometrical datum of the blade is given in Table 3. The last column in Table 3 is the blade airfoils. The first segment near the blade root is designed as cylinder with diameter 2.0m. The second segment between 0.1*R* and the 0.2*R* is designed as the transition shape. The rest segments are designed as the S serial airfoils.

Table 2 The geometrical and mass datum of the wind turbine rotor

Wind turbine rotor		Blade		Hub	
Diameter/m	Weight/ton	Length/m	Weight/ton	Diameter/m	Weight/ton
80	28.505	38.5	6.1	3.0	10.205

Table 3 The geometrical parameters of the blade (Blade length R=38.5m)

Ratio between r and R	Distance from blade root r/m	Chord length c/m	Blade twist angle β/^{0}	Airfoil type
0.1	3.85	2.0	0	Cylinder
0.2	7.7	4.14	13.67	S815
0.3	11.55	3.21	8.95	S815
0.4	15.4	2.46	5.08	S814
0.5	19.25	2.03	2.61	S814
0.6	23.1	1.54	0.90	S830
0.7	26.95	1.34	-0.34	S830
0.8	30.8	1.18	-1.28	S830
0.9	34.65	0.98	-2.01	S831
1.0	38.5	0.89	-2.61	S832

Note: r is the distance from blade root to current blade section. c is the blade chord length. β is the blade twist angle at r location.

The coordinate transformation method [10] is utilized to compute the angles between the wind direction and the blade coordinates. After the angles are obtained, the aerodynamic forces of wind on blades will be computed with commercial CFD code. The NURBS is used to build the irregular blade surface. The pressure flow field is modeled according to the blade shape. The length, width, and depth of the pressure flow field are set as 5 times of the blade length, 3 times of the blade width and 3 times of the blade depth, respectively. The whole pressure flow field and the mesh of one cross section are shown in Fig. 4. The blade is located in the middle of the pressure flow field. The grid size near the blade surface is subdivided into smaller sections than that of the grids far away from the blade surface. There are total 76694 nodes and 146505 grids on the blade surface.

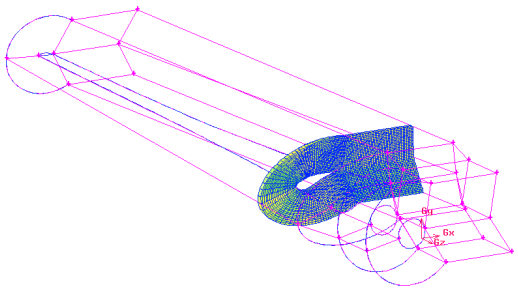

The Hoisting Forces Computation

Fig. 4 The pressure flow field and the mesh of one cross section near the blade root

Due to the good aerodynamic characteristics of the blade, the wind speed should be no more than 8m/s for the blade hoisting process. The wind speed is set as 8m/s and the Spalart-Allmaras turbulence model [11] is used for computation. No-slip boundary condition is used for blade and pressure far field is for the surrounding boundary. The air is assumed to be incompressible and the density is set as 1.225kg/m^3. The atmosphere pressure is set as 101325Pa. The 2-order upwind momentum and SIMPLER algorithm is adopted to compute the pressure-velocity coupling.

For blade 1, the azimuth angle is 0^0, the blade pitch angle range is [-90^0, 90^0] and the yaw angle range is [0^0, 360^0]. Referring to the rotor coordinate system, the hoisting forces Fx, Fy and Fz are computed, respectively. Fz is equal to the blade weight plus the aerodynamic forces in z direction. The change process of the hoisting forces Fx, Fy and Fz of blade 1 are illustrated in Fig. 5, Fig. 6 and Fig. 7, respectively. The two boldface lines denote the hoisting forces with $\pm 90^0$ pitch angles. The thick

dashed line denotes the hoisting forces with 0^0 pitch angle. In view of Fig. 5, the hoisting forces *Fx* vary over a wide range with respect to the pitch angle 0^0, $\pm30^0$ and $\pm60^0$ in one yaw circle. The nearer the pitch angle is to 0^0, the bigger the hoisting forces *Fx* changes. On the contrary, the hoisting forces *Fx* of blade 1 with pitch angle $\pm90^0$ change slightly and the hoisting forces are relatively small. Obviously, to reduce the hoisting forces and keep the stability of the blade hoisting process, the pitch angle of the blade 1 is suggested to be set as $\pm90^0$ in the hoisting process.

In Fig. 6, the hoisting forces *Fy* of blade 1 change slightly and they are relatively small with 0^0 pitch angle in one yaw circle whereas the hoisting forces *Fy* vary over a wide range with the pitch angle $\pm30^0$, $\pm60^0$ and $\pm90^0$. It is a contradiction to make hoisting forces *Fx* and *Fy* of the blade 1 change slightly with the same pitch angle. In Fig. 7, the hoisting forces *Fz* of blade 1 change a great deal whatever the pitch angle is in one yaw circle. For each pitch angle in one yaw circle, there exist one maximal force and one minimal force *Fz*. Though the minimal forces *Fx*, *Fy* and *Fz* of blade 1 can not be obtained with the same pitch angle and yaw angle, the small forces *Fx*, *Fy* and *Fz* in one yaw circle can be obtained at the same yaw angle interval and the same pitch angles. It is found that the *Fx*, *Fy* and *Fz* change slightly when the yaw angle is at the interval $[150^0, 210^0]$ and the pitch angles are equal to $\pm90^0$.

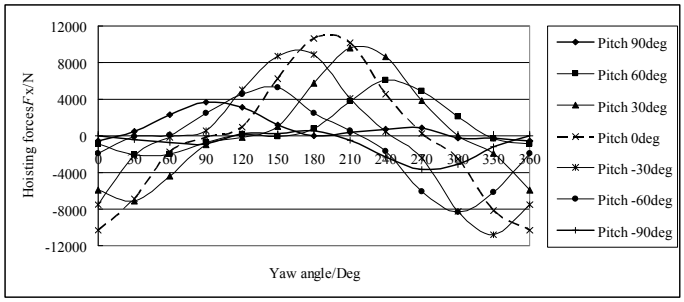

Fig. 5 The change of the hoisting forces *Fx* of blade 1 according to positions

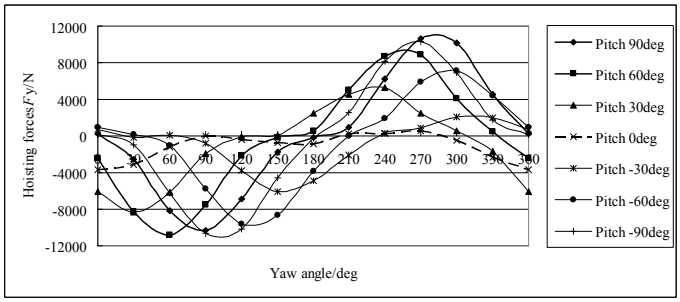

Fig. 6 The change of the hoisting forces *Fy* of blade 1 according to positions

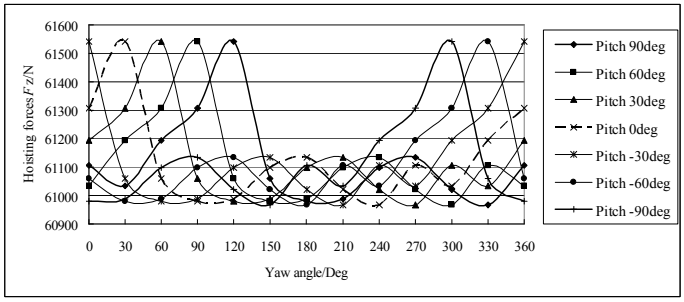

Fig. 7 The change of the hoisting forces *Fz* of blade 1 according to positions

Table 4 The maximal and minimal hoisting forces and corresponding positions of three blades

F/N & positions	Fx_{max}/N	Fx_{min}/N	Fy_{max}/N	Fy_{min}/N	Fz_{max}/N	Fz_{min}/N
	(A, P, Y)	(A, P, Y)	(A, P, Y)	(A, P, Y)	(A, P, Y)	(A, P, Y)
Blade 1	-10796.6	-29.3	-10793.6	-29.3	61539.9	60967.9
	(0^0,-30^0, 330^0)	(0^0,90^0, 180^0) (0^0,-90^0, 0^0)	(0^0,60^0, 60^0)	(0^0, 0^0, 90^0)	See Fig.7	See Fig.7
Blade 2	-11263.2	-2.1	3202	-13.6	66227.1	56940.7
	(-120^0, 0^0, 0^0)	(-120^0, -90^0, 240^0)	(-120^0, 30^0, 0^0)	(-120^0, 0^0, 240^0)	(-120^0, 30^0, 330^0)	(-120^0, 90^0, 60^0)
Blade 3	-11263.2	2.1	2902	21.6	64223.2	54557.7
	(120^0, 0^0, 360^0)	(120^0,90^0, 60^0)	(120^0,-60^0, 210^0)	(120^0,60^0, 210^0)	(120^0,60^0, 120^0)	(120^0,30^0, 330^0)

The hoisting forces of blade 2 and blade 3 in Fig. 1 are also computed. The maximum and minimum hoisting forces of the three blades and their corresponding positions are shown in Table 4. It is interesting that the change of these forces also change gradually with the yaw angle interval [150^0, 210^0] and $\pm 90^0$ pitch angles. To reduce the rotor hoisting forces, the pitch angles of three blades can be taken as different values, for example, the yaw angle of blade 1 takes values from the interval [180^0, 210^0] whereas blade 2 and blade 3 take values from the interval [150^0, 180^0].

Conclusions

The hoisting forces of one 38.5m blade are computed with CFD method. The computation model is constructed with the blade geometrical data, blade positions and wind conditions. The blades positions are concluded by the blade pitch angle, azimuth angle and rotor yaw angle. The coordinate transformation method is used to compute the angle between the wind direction and the blade coordinate axes. The hoisting forces of three blades at 252 positions are computed and analyzed. The maximal and minimal hoisting forces of each blade in a three dimension coordinate system are found and the corresponding blade positions are obtained. Suggestions are given to reduce the blades hoisting forces and increase the safety of the hoisting process.

In the computation, the boundary conditions are simple. Therefore, the computational results may deviate from the actual hoisting forces. The boundary conditions will be enhanced to compute the accurate hoisting forces. Various wind conditions will also be tried to compute the hoisting forces of blades and rotor in the future.

Acknowledgements

The authors acknowledge Emily Moder for checking the paper, and the fund supported by “the Fundamental Research Funds for the Central Universities” (Grant No.12MS48).

References

[1] C. Sicot, P. Devinant, S. Loyer and J. Hureau, Rotational and turbulence effects on a wind turbine blade, Journal of Wind Engineering and Industrial Aerodynamics. 96(2008) 1320-1331.

[2] P. Fuglsang and H.A. Madsen, Optimization method for wind turbine rotors, Journal of Wind Engineering and Industrial Aerodynamics. 80(1999) 191-206.

[3] J. Bystryk, P. E. Sullivan, Small wind turbine power control in intermittent wind gusts, Journal of Wind Engineering and Industrial Aerodynamics. 99(2011) 624-637.

[4] GB/T19568-2004, Assembly and installation standards of wind turbine (in Chinese), China Zhijian Publishing House, Beijing, 2004, pp.4-5.

[5] Y. Bai, W. Wang, J. J. Zhang, et, al, Installation technology of offshore wind turbine, The 2nd Academic Symposium on China Ocean Energy, Harbin, China, 2009, pp.112-8.

[6] L. Cochran, R. Derickson, A physical modeler's view of Computational Wind Engineering, Journal of Wind Engineering and Industrial Aerodynamics. 99(2011) 139-153.

[7] W. He, Blade aerodynamic design and numerical simulation of large scale wind power generator, Wuhan University Press, Wuhan, 2009, pp.67-71.

[8] D. M. Somers, the S814 and S815 Airfoils: National Renewable Energy Laboratory, 1991.

[9] D. M. Somers, the S830 and S831 Airfoils: National Renewable Energy Laboratory, 2001.

[10] D. Hearn, M. P. Baker, Computer graphics with OpenGL, 3rd edition, Pearson Education Inc., Boston, 2004, pp.218-220.

[11] Y. W. Liu, L. P. Lu, L. Fang, F. Gao, Modification of Spalart-Allmaras model with consideration of turbulence energy backscatter using velocity helicity, Physics Letters. 375(2011) 2377-2381.